

BEYOND ACCURACY: A STABILITY-AWARE METRIC FOR MULTI-HORIZON FORECASTING

CHUTIAN MA, GRIGORII POMAZKIN, GIACINTO PAOLO SAGGESE, AND PAUL SMITH

ABSTRACT. Traditional time series forecasting methods optimize for accuracy alone. This objective neglects temporal consistency, in other words, how consistently a model predicts the same future event as the forecast origin changes. We introduce the forecast accuracy and coherence score (forecast AC score for short) for measuring the quality of probabilistic multi-horizon forecasts in a way that accounts for both multi-horizon accuracy and stability. Our score additionally allows user-specified weights to balance accuracy and consistency requirements. As an example application, we implement the score as a differentiable objective function for training seasonal auto-regressive integrated models and evaluate it on the M4 Hourly benchmark dataset. Results demonstrate substantial improvements over traditional maximum likelihood estimation. Regarding stability, the AC-optimized model generated out-of-sample forecasts with 91.1% reduced vertical variance relative to the MLE-fitted model. In terms of accuracy, the AC-optimized model achieved considerable improvements for medium-to-long-horizon forecasts. While one-step-ahead forecasts exhibited a 7.5% increase in MAPE, all subsequent horizons experienced an improved accuracy as measured by MAPE of up to 26%. These results indicate that our metric successfully trains models to produce more stable and accurate multi-step forecasts in exchange for some degradation in one-step-ahead performance.

CONTENTS

1. Introduction	1
2. Related Work	3
3. Proposed Framework	4
4. Experiments	11
5. Conclusion	20
6. Future Directions	21
References	22

1. INTRODUCTION

We consider a setting where multi-horizon, probabilistic forecasts are issued at regular intervals. For example, one may consider the chance of rain on any given day over the next week in a particular locale. With the advance of each day, we observe an outcome we previously did not have access to, and, at the outer reach of our forecasting horizon, we record an initial forecast. For the days in between

Code available at https://github.com/causify-ai/beyond_accuracy.

the newly observed outcome and the limit of the forecasting horizon, we record updated forecasts. These forecast updates typically reflect at least two things:

- (1) New information not previously available (e.g., new weather observations).
- (2) The reduction (by one time step) of forecast horizon, and hence, *ceteris paribus*, forecast uncertainty.

1.1. Stability of Forecast Revision over Time. In the setting where the forecast horizon is fixed (e.g., next-day weather forecasts), the problem of forecast accuracy is well-studied and typically quantified using proper scoring rules. In contrast, the focus of our work is on *forecast stability*, which has received comparatively little attention. To relate this concept back to our weather forecasting example, suppose that today is a Sunday and we are considering the daily chance-of-rain forecasts for the next seven days. Our initial forecast for *next* Sunday’s chance of rain is a seven-day ahead forecast, at the outer reach of our forecast curve. Common experience would recommend that we take this forecast less seriously than, say, the next-day chance-of-rain forecast that we will have access to on Saturday, the day before next Sunday. As the days advance from Sunday through Saturday, we observe an updated chance-of-rain forecast for next Sunday, and by the time we reach Sunday and observe the outcome, we will have accumulated seven sequential probabilistic forecasts.

What we propose to capture is a measure of the *stability*, or lack thereof, of these sequential forecast updates. Through several examples below, we illustrate that forecast stability is a meaningful concept to measure and can play an important role in discriminating between two competing sets of forecasts. All things being equal—a concept we will rigorously define—we would prefer sequential forecasts that appear harmonious rather than conflicting.

Additionally, we propose incorporating forecast stability in a loss function while training time series models, with the extent to which stability is weighted tailored to the forecasting needs for the problem at hand.

1.2. Time-based Forecast Weights for Decision Problems. In addition to capturing forecast stability, we propose incorporating problem-tailored forecast-horizon based weightings in forecast quality metrics. Using horizon-based weights is motivated by the way multi-horizon forecasts may be used in various decision-making problems. In other words, the importance of time weighting is not necessarily inherent in the forecasting procedure itself, but rather in how the forecasts are used. To return to our weather example, we note that the decision about whether to carry an umbrella outside on Sunday may be postponed to the last minute, assuming one has easy access to an umbrella. A decision about whether to wash a car might be made based upon a one or two day rain forecast. However, decisions around contingency planning for an outdoor event may need to be made much further in advance. If such intended usage is captured in a forecast quality metric, then we may better judge forecast quality for a given decision problem. When we also have control over the way forecasts are made, we may then in turn use this metric as part of the training optimization procedure.

1.3. Comprehensive Time Series Metrics. In the sequel, we propose a comprehensive time series metric framework that is both natural and flexible enough to capture a wide range of time series properties desirable in practice for effectively utilizing probabilistic multi-horizon forecasts in making decisions.

Remark (Desiderata). The following properties are desirable of a metric, all else being equal:

- (1) The more accurate a forecast, the better.
- (2) Accuracy of forecasts immediately prior to a decision point are more important than forecasts too far ahead of or after a decision point (note that a decision point may be well in advance of the observed outcome).
- (3) The less revision in a forecast, the better.

In many applications, decisions must be made at some point between the forecast origin and the target time. Forecasts issued long before the decision point may require down-weighting or discounting, while those close to the decision should receive greater emphasis. Introducing a weighting scheme along the forecast path allows one to focus on accuracy and stability in the periods that matter most.

Stability is also critical when early action is possible. If the sequence of forecasts for a target is sufficiently stable, then decision makers can act with greater confidence on early forecasts. Conversely, highly volatile forecast sequences may delay action or require more robust risk management.

Together, these considerations motivate a framework in which accuracy and stability are quantified separately and combined in a weighted metric-space score, allowing both dimensions to inform probabilistic multi-step decision-making.

2. RELATED WORK

Forecast stability remains an understudied area in the forecasting literature. Some studies [3] touch upon what is termed “vertical stability”, focusing on how forecasts for a given target period vary when generated from different lead times.

Recent work [6] has introduced a new measure of forecast stability, namely *congruence*, which is a measure that directly quantifies vertical forecast stability by computing the variance of forecasts made at different origins for the same target time. However, the extension of this concept to probabilistic forecasts remains unexplored.

One of the first attempts to assess probabilistic forecast stability appears in Zanotti [10], who introduces the Multi-Quantile Change (MQC) metric. MQC measures instability by tracking changes across a set of predictive quantiles, providing a model-agnostic and scale-free evaluation. However, because it relies on a finite set of quantiles rather than the full predictive distribution, MQC cannot capture all aspects of distributional change, especially those occurring between or beyond the chosen quantile levels.

Klee and Xia [4] emphasize that, in production supply-chain environments, planners value stable forecasts. Their study focuses on model-induced stability (forecast variance when inputs are fixed) rather than the origin-to-target stability we examine, but it nevertheless highlights the operational importance of consistent forecasts for demand planners. Genov et al. [1] examine the operational implications of forecast stability in a decision-making system subject to switching costs (costs of changing a policy because the forecast changed). They show that in contexts where frequent policy adjustments incur real costs, more stable forecasts deliver better downstream performance.

3. PROPOSED FRAMEWORK

3.1. Problem definition. Consider a multi-horizon forecasting scenario where the forecaster receives new information at each timestamp t . The information available to the forecaster at time t is denoted as $\mathcal{Z}_t = (Z_1, Z_2, \dots, Z_t)$. Z_t represents the new information that arrives at t , which contains the newly realized value of the target time series and any covariates that become known at time t . The forecaster then generates m -step-ahead forecasts using all relevant information available up to (and including) time t . The m -step-ahead forecasts issued at *origin time* t are denoted as $\hat{y}_{t+1|t}, \hat{y}_{t+2|t}, \dots, \hat{y}_{t+m|t}$, where the subscripts $t+j$ correspond to the forecast target time and t corresponds to the forecast origin. We assume the m -step-ahead forecasts are sampled from a joint probability distribution $f_t(\hat{y}_{t+1|t}, \hat{y}_{t+2|t}, \dots, \hat{y}_{t+m|t})$.

Collecting forecast distributions issued at origin times $t = 1, \dots, n$ given the realizations Z_t , we arrange them into the following a $n \times 1$ matrix.

Definition 3.1 (Forecast Ensemble Given One Realization). We call the matrix of multivariate probability distributions in (1) a forecast ensemble given realization \mathcal{Z} .

$$(1) \quad \mathbf{F}|\mathcal{Z} = \begin{bmatrix} f_1(\hat{y}_{2|1}, \hat{y}_{3|1}, \dots, \hat{y}_{m+1|1}|Z_1) \\ f_2(\hat{y}_{3|2}, \hat{y}_{4|2}, \dots, \hat{y}_{m+2|2}|Z_2) \\ \vdots \\ f_n(\hat{y}_{n+1|n}, \hat{y}_{n+2|n}, \dots, \hat{y}_{n+m|n}|Z_n) \end{bmatrix}$$

For each $1 \leq t \leq n$, we can draw samples of the next m step-ahead forecasts from the joint distribution f_t . We stack the generated samples together into an $n \times m$ matrix.

$$(2) \quad \begin{bmatrix} \hat{y}_{2|1} & \hat{y}_{3|1} & \hat{y}_{4|1} & \cdots & \hat{y}_{m+1|1} \\ \hat{y}_{3|2} & \hat{y}_{4|2} & & & \vdots \\ \hat{y}_{4|3} & & \ddots & & \\ \vdots & & & & \\ \hat{y}_{n+1|n} & \cdots & & & \hat{y}_{n+m|n} \end{bmatrix}.$$

We call (2) a forecast sample ensemble given realization \mathcal{Z} . When there is no risk of confusion, we may simply call it a forecast ensemble.

Forecast stability concerns how consistently a forecasting system predicts the *same* future event as the forecast origin changes.

Qualitatively speaking, a forecasting method is said to be *stable* if the revisions between forecasts with the same target time are small as new information arrives. Conversely, large updates between successive forecasts indicate instability: the system repeatedly alters its expectation of the same future target. Below we describe how to measure such variation in a natural way so as to quantify forecast stability.

Definition 3.2 (Vertical Stability). The anti-diagonals in the forecast sample ensemble (2) represent forecasts issued at different origins targeting the same timestamp, i.e., the entries

$$(3) \quad \{\hat{y}_{t|t-m}, \hat{y}_{t|t-m+1}, \dots, \hat{y}_{t|t-1}\}$$

are forecasts targeting the time t issued at different origins $t-m, t-m+1, \dots, t-1$, respectively. Each anti-diagonal therefore collects the sequence of forecast revisions

for a particular target time. Vertical stability refers to the volatility of the sequence (3), measured by its variance averaged over t .

In applications such as supply chain demand forecasting, having demand forecasts of the same target day issued at different origins show great variability can be problematic due to the decision making costs. Certain decisions made based on previous forecasts, e.g., ordering supplies from a supplier, incur real costs and may not be reversible. Having greater volatility in forecasts targeting the same timestamp can therefore make decision making difficult and reduce the decision maker's confidence in the forecasts. In such situations, stability, in addition to accuracy, is a desirable property for forecasts targeting the same timestamp. This kind of stability was first raised in [3] and named *vertical stability*.

Definition 3.3 (Horizontal Stability). Rows of the forecast sample ensemble (2) correspond to forecasts issued at a fixed origin time, i.e., all forecasts generated at time t with horizons ranging from 1 to m :

$$\mathbf{F}_{t,:} = [\hat{y}_{t+1|t}, \hat{y}_{t+2|t}, \dots, \hat{y}_{t+m|t}].$$

This row therefore represents the *forecast trajectory* or *forecast vector* produced at a single origin. Stability along this direction is called Horizontal stability as proposed in [3].

3.2. Measuring the distance between forecast distributions. Consider the space of all probability distributions. We may choose a metric which evaluates the discrepancy between two distributions, including their center, spread, and overall shape.

Example 3.1 (CRPS). Given two 1-dimensional random variables X, Y with probability distributions F and G respectively, we can define the metric d^2 to be

$$(4) \quad d^2(F, G) = \mathbb{E}_{F, G} |X - Y| - \frac{1}{2} \mathbb{E}_F |X - X'| - \frac{1}{2} \mathbb{E}_G |Y - Y'|$$

where X' is an independent and identical copy of X . Let δ_y be the Dirac distribution supported at the true outcome value y . Then we may measure the accuracy of a forecast distribution by $d^2(\hat{Y}, \delta_y)$, which is exactly the *Continuous Ranked Probability Score (CRPS)* [2]. For 1-dimensional random variables, *CRPS* can be expressed alternatively by

$$(5) \quad CRPS(F, y) = \int (F(x) - \mathbb{1}_{x > y}(y))^2 dy.$$

Example 3.2 (Energy Score and Distance). In higher dimensional cases, we replace the absolute value in (4) by L^2 norm, i.e.

$$D^2(F, G) = \mathbb{E}_{X \sim F, Y \sim G} \|X - Y\| - \frac{1}{2} \mathbb{E}_{X, X' \sim F} \|X - X'\| - \frac{1}{2} \mathbb{E}_{Y, Y' \sim G} \|Y - Y'\|$$

where $\|(x_1, \dots, x_n)\| = (\sum x_i^2)^{\frac{1}{2}}$ is the L^2 norm. Then we recover the squared *Energy Distance* [7]. Suppose the random variable $Y \sim G$ is realized and the realized value is y . One may view the realization as a Dirac measure supported at y . Substituting it into G , we recover the *Energy Score* [2]

$$(6) \quad ES(F, y) = \mathbb{E}_{X \sim F} \|X - y\| - \frac{1}{2} \mathbb{E}_{X, X' \sim F} \|X - X'\|.$$

Note that the energy score is reduced to CRPS in the 1-dimensional case.

Choosing a suitable metric allows us to study how the sequence of forecast revisions evolves as the forecast origin changes. To be precise, we fix a target time t and consider two sequences of forecast paths $\hat{y}_{t|s}$ and $\hat{y}'_{t|s}$, both aimed at predicting the same realization at time t . Let y denote the true outcome of the target.

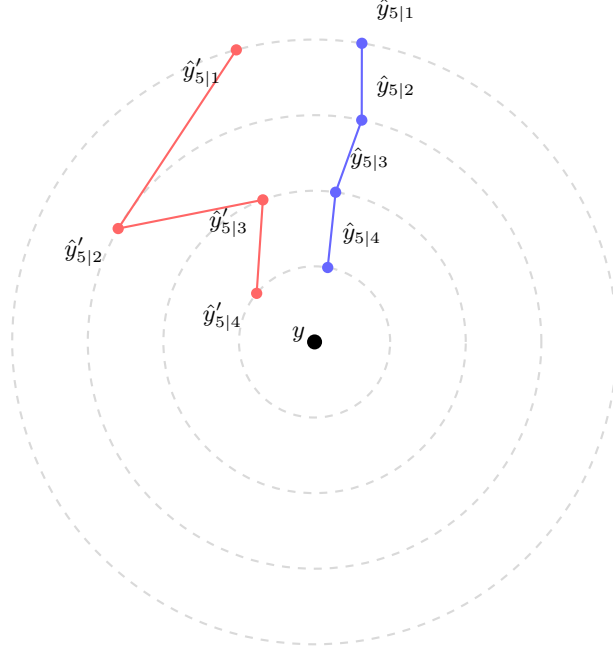


FIGURE 1. Illustration of two forecast sequences.

Suppose that both sequences have the same accuracy at every revision, in the sense that

$$d(\hat{y}_{t|s}, \delta_y) = d(\hat{y}'_{t|s}, \delta_y) \quad \text{for all valid origins } s.$$

As shown in Figure 1, even with equal accuracy, the *paths* traced by the two sequences may differ in volatility. We prefer the sequence $\{\hat{y}_{t|s}\}$ because its path is less volatile. This motivates separating the notions of *accuracy* (closeness to the truth) and *stability* (smoothness of the forecast path).

Definition 3.4 (Accuracy score defined on joint distributions). Our score consists of two components, an accuracy component $\text{Acc}(F|\mathcal{Z})$ which measures the accuracy of the multi-horizon forecasts and a stability component $\text{Stb}(F|\mathcal{Z})$ which measures the smoothness between successive forecasts.

The accuracy score is defined via the energy score. Let

$$y_{\text{true}}(t) = (y_{t+1}, \dots, y_{t+m})$$

denote the true values of the next m target values. Let

$$\hat{Y}_{\text{pred}}(t) = (\hat{y}_{t+1|t}, \dots, \hat{y}_{t+m|t})$$

be the multivariate random variable representing the next m step forecasts. Then the weighted energy score of the multi-step forecast distribution f_t given true outcomes $y_{\text{true}}(t)$ is equal to

$$(7) \quad \text{ES}(f_t, y_{\text{true}}(t)) = \mathbb{E} \|\hat{Y}_{\text{pred}}(t) - y_{\text{true}}(t)\|_w - \frac{1}{2} \mathbb{E} \|\hat{Y}_{\text{pred}}(t) - \hat{Y}'_{\text{pred}}(t)\|_w$$

where $\hat{Y}'_{\text{pred}}(t)$ is an independent copy of $\hat{Y}_{\text{pred}}(t)$, i.e., $\hat{Y}'_{\text{pred}}(t)$ has the same distribution as but is independent of $\hat{Y}_{\text{pred}}(t)$. Here $\|\cdot\|_w$ is a weighted version of Euclidean distance:

$$(8) \quad \|X - Y\|_w = \left(\sum_i w_i |X_i - Y_i|^2 \right)^{\frac{1}{2}}$$

with $w_i \geq 0$. The purpose of the weight w is to assign different levels of importance to optimizing the accuracy of short-range forecasts versus long-range forecasts. For example, a forecast error targeting tomorrow may be considered more severe than the same error for a forecast targeting one month ahead. The *accuracy score* is defined by

$$(9) \quad \text{Acc}(F|\mathcal{Z}) = \frac{1}{n} \sum_{t=1}^n \text{ES}(f_t, y_{\text{true}}(t)).$$

It measures the average accuracy across all forecast origin times

We now proceed to define the stability measurement of our forecast ensemble. Formally, denote marg_X to be the operator that marginalizes a joint distribution $f(X, Y)$ over X . On random variables $X, Y \sim f(x, y)$, marg_X is defined by projecting onto X :

$$(10) \quad \text{marg}_X(X, Y) = Y.$$

Without risk of confusion, we may define it on the joint distribution $f(x, y)$ by

$$(11) \quad (\text{marg}_X f)(y) = \int f(x, y) dx.$$

Definition 3.5 (Stability score defined on joint distribution given realization). The *stability score* measures the smoothness of the forecast revision path, i.e., how much the forecasts targeting the same timestamp change between successive origins. To be precise, at time t we have the next m step forecasts

$$\hat{Y}_{\text{pred}}(t) = (\hat{y}_{t+1|t}, \dots, \hat{y}_{t+m|t}) \sim f_t$$

and at time $t + 1$ we have

$$\hat{Y}_{\text{pred}}(t + 1) = (\hat{y}_{t+2|t+1}, \dots, \hat{y}_{t+m+1|t+1}) \sim f_{t+1}.$$

Note that $\hat{Y}_{\text{pred}}(t)$ aims at predicting $t + 1$ up to $t + m$, while $\hat{Y}_{\text{pred}}(t + 1)$ aims at predicting $t + 2$ up to $t + m + 1$. In order to compare the forecasts targeting the same timestamps, we marginalize out the non-overlapping components of $\hat{Y}_{\text{pred}}(t)$ and $\hat{Y}_{\text{pred}}(t + 1)$, i.e.,

$$\text{marg}_{\hat{y}_{t+1|t}} \hat{Y}_{\text{pred}}(t) = (\hat{Y}_{t+2|t}, \dots, \hat{Y}_{t+m|t})$$

and

$$\underset{\hat{y}_{t+m+1|t+1}}{\text{marg}} \hat{Y}_{\text{pred}}(t+1) = (\hat{Y}_{t+2|t+1}, \dots, \hat{Y}_{t+m|t+1}).$$

After marginalization, the difference between forecast distributions issued at t and $t+1$ can be measured by the squared weighted energy distance

$$(12) \quad D^2(\underset{\hat{Y}_{t+1|t}}{\text{marg}} f_t, \underset{\hat{Y}_{t+m+1|t+1}}{\text{marg}} f_{t+1}) = \mathbb{E} \left\| \underset{\hat{Y}_{t+1|t}}{\text{marg}} \hat{Y}_{\text{pred}}(t) - \underset{\hat{Y}_{t+m+1|t+1}}{\text{marg}} \hat{Y}_{\text{pred}}(t+1) \right\|_w \\ - \frac{1}{2} \mathbb{E} \left\| \underset{\hat{Y}_{t+1|t}}{\text{marg}} \hat{Y}_{\text{pred}}(t) - \underset{\hat{Y}_{t+1|t}}{\text{marg}} \hat{Y}'_{\text{pred}}(t) \right\|_w \\ - \frac{1}{2} \mathbb{E} \left\| \underset{\hat{Y}_{t+m+1|t+1}}{\text{marg}} \hat{Y}_{\text{pred}}(t+1) - \underset{\hat{Y}_{t+m+1|t+1}}{\text{marg}} \hat{Y}'_{\text{pred}}(t+1) \right\|_w.$$

We average over all pairs of successive forecast origins to get an overall stability score

$$(13) \quad \text{Stb}(F|\mathcal{Z}) = \frac{1}{n-1} \sum_{t=1}^{n-1} D^2(\underset{\hat{Y}_{t+1|t}}{\text{marg}} f_t, \underset{\hat{Y}_{t+m+1|t+1}}{\text{marg}} f_{t+1}).$$

This characterizes the expected stability score averaged over all forecast samples generated for a single realization.

Definition 3.6 (Forecast Accuracy and Coherence (AC) Score). The *forecast accuracy and coherence score*, or *AC score* for short, is defined as a weighted combination of accuracy and stability scores:

$$(14) \quad S_{\text{AC};\lambda}(F|\mathcal{Z}) = \text{Acc}(F|\mathcal{Z}) + \lambda \text{Stb}(F|\mathcal{Z})$$

for some non-negative weight λ . Typically we suppress the dependence of λ in our notation, using S_{AC} for brevity.

Remark. The metric evaluates forecast quality based solely on the resulting distributions, without assuming how those forecasts are produced. This can be applied to diverse types of multi-horizon forecasting models, for example

- *Iterative forecasting:* Multi-step forecasts generated by repeatedly applying one-step-ahead models, common in classical time series methods and transformer-based architectures.
- *Direct multi-horizon forecasting:* Models trained to produce all forecast horizons simultaneously, which is commonly used in modern neural architectures.
- *Skeleton-based forecasting:* Generating forecasts at sparse key horizons (e.g., $h \in \{24, 48, 72\}$ for hourly data) and using interpolation, extrapolation, or learned smoothing to obtain intermediate forecasts.
- *Attention-based architectures:* Transformer models like Temporal Fusion Transformer that use self-attention mechanisms to capture temporal dependencies and generate multi-horizon forecasts.

3.3. Empirical Approximation. The scores defined in section 3.2 can be computed empirically with samples. Suppose the forecaster makes forecasts on a rolling basis. At each time t , the forecaster utilizes the most up-to-date information at t , namely Z_t , to generate k sample paths $(\hat{y}_{t+1|t}^{(i)}, \dots, \hat{y}_{t+m|t}^{(i)})$, $1 \leq i \leq k$, each of which

forecasts the next m step target values. When the rolling forecasting procedure finishes, we have k forecast sample ensembles of the form (2). We illustrate how to compute the accuracy score (9) and the stability score (13) empirically based on the sample ensembles. The energy score (7) can be computed empirically by (15)

$$(15) \quad \frac{1}{k} \sum_{i=1}^k \left(\sum_{j=1}^m w_j |\hat{y}_{t+j|t}^{(i)} - y_{t+j}|^2 \right)^{\frac{1}{2}} - \frac{1}{k(k-1)} \sum_{1 \leq i_1 < i_2 \leq k} \left(\sum_{j=1}^m w_j |\hat{y}_{t+j|t}^{(i_1)} - \hat{y}_{t+j|t}^{(i_2)}|^2 \right)^{\frac{1}{2}}$$

Similarly, the energy distance (12) between successive forecasts can be computed empirically by

$$(16) \quad \begin{aligned} & \frac{1}{k} \sum_{i=1}^k \left(\sum_{j=2}^m w_j |\hat{y}_{t+j|t}^{(i)} - \hat{y}_{t+j|t+1}^{(i)}|^2 \right)^{\frac{1}{2}} \\ & - \frac{1}{k(k-1)} \sum_{1 \leq i_1 < i_2 \leq k} \left(\sum_{j=2}^m w_j |\hat{y}_{t+j|t}^{(i_1)} - \hat{y}_{t+j|t}^{(i_2)}|^2 \right)^{\frac{1}{2}} \\ & - \frac{1}{k(k-1)} \sum_{1 \leq i_1 < i_2 \leq k} \left(\sum_{j=2}^m w_j |\hat{y}_{t+j|t+1}^{(i_1)} - \hat{y}_{t+j|t+1}^{(i_2)}|^2 \right)^{\frac{1}{2}} \end{aligned}$$

Then, the accuracy score (9) and the stability score (13) are computed by averaging (15) and (16) over time t respectively.

Remark (Point Forecast as a Special Case). The forecast AC score can be extended to evaluating point forecasts. In fact, the point estimate \hat{y} may be viewed as a Dirac distribution supported at \hat{y} . Thus the empirical formula of accuracy score (15) becomes

$$(17) \quad Acc(F|Z) = \frac{1}{n} \sum_{t=1}^n \left(\sum_{j=1}^m w_j |\hat{y}_{t+j|t} - y_{t+j}|^2 \right)^{\frac{1}{2}}$$

and (16) becomes

$$(18) \quad Stb(F|Z) = \frac{1}{n-1} \sum_{t=1}^{n-1} \left(\sum_{j=2}^m w_j |\hat{y}_{t+j|t} - \hat{y}_{t+j|t+1}|^2 \right)^{\frac{1}{2}}.$$

3.4. Expected AC Score Given a Data Generation Process. So far, we have defined the accuracy and stability score where all samples of forecasts are conditioned on the same realization. This applies to use cases where the experiment that generated the realized time series is done only once, e.g. sales numbers of a specific retail shop. In some situations, there are multiple observed test subjects, each yielding their own realized time series, all subject to the same underlying mechanism. Consider the following example where someone working for Walmart has access to the sales data from Walmart stores across the nation and their goal is to choose a single forecast model that achieves the best overall performance for all stores. One might assume that the sales time series from all stores are generated

by the same data generation process with noise. This motivates extending the AC score conditioned on a realization to the following.

Definition 3.7 (Forecast AC score given data generating process). Suppose the underlying data generation process is known. We define the expected stability score as

$$(19) \quad S_{AC}(F) = \mathbb{E}_{\mathcal{Z}}[S_{AC}(F|\mathcal{Z})].$$

The expectation is taken over all possible realizations based on their likelihood under the data generation process. This expected score characterizes how well one expects the forecast model to work on a random test subject which follows the same data generation process as the time series which the model was trained on.

3.5. The Choice of Weights. In this subsection, we discuss the potential choice of the weights w_j in (8). Not all forecast updates matter equally. Early forecasts are highly uncertain and usually have limited operational impact, while updates made close to a decision point directly affect actions such as ordering, scheduling, or resource allocation. Therefore, both accuracy and stability should be weighted more heavily near a decision point, where errors and unnecessary revisions are most costly. Introducing time-dependent weights allows the score to reflect these practical priorities: emphasizing accuracy near but ahead of decision points, penalizing last-minute volatility, and aligning the evaluation with the timing of real decisions.

By allowing accuracy and stability to use separate weighting functions, the framework can be adapted to different operational contexts in which the value of precise or stable forecasts changes over time.

For a fixed target time T and the earliest origin denoted as i_{\min} , let the decision time τ be a time between the earliest origin and the target time, i.e., $i_{\min} \leq \tau < T$. Then, it is convenient to define the distance to the the decision time from the origin as $u = |i - \tau|$ and to define a corresponding weighting function $w(u)$. Similarly, define the horizon h as the distance from origin to target time, $h = T - i$, and the corresponding weighting function $w(h)$. Depending upon the operational context, one representation may be more natural than the other, i.e., a representation based on distance from the origin to the decision time versus a representation based on distance from the origin to the target time. Below, we will develop the case for $w(h)$; that for $w(u)$ is analogous.

To ensure a meaningful and interpretable evaluation, the weighting function should satisfy a few basic properties:

- (1) Non-negativity: $w(h) \geq 0$.
- (2) Normalization: $\sum_h w(h) = 1$. Ensures compatibility across horizons and across datasets.
- (3) Monotonicity toward the target time (optional): weights increase as we approach the decision point, $w(h_1) \leq w(h_2)$ whenever $h_1 > h_2$. It is assumed that later forecasts are more consequential. However, the framework allows for alternative shapes (e.g., U-shaped) depending upon domain needs.

The weighting function is a hyperparameter; one is free to choose one that fits a use case best. Below we summarize several widely used functional forms:

- (1) Exponential: $w(h) = e^{-\alpha h}$
- (2) Linear: $w(h) = a + bh, b < 0$
- (3) Hyperbolic: $w(h) = \frac{1}{1+\beta h}$

(4) Inverse-variance: $w(h) = \frac{1}{\text{Var}(f_h)}$

(5) Piecewise: weights change at predefined horizons (e.g., operational cycles)

The functional forms listed above specify the relative shape of the weights but do not enforce that they sum to one. In practice, the weights should be normalized.

Accuracy and stability capture different aspects of forecast quality. Accuracy measures closeness to the true target, while stability measures temporal consistency across origins. Their operational relevance may differ: late revisions can have high costs, affecting stability, while accuracy may be more relevant across all horizons. The proposed framework allows the use of separate weighting functions, $w(h)$ for accuracy and $w'(h)$ for stability, to reflect these differences. In applications where the same importance applies, the same function can be used for both.

4. EXPERIMENTS

In this section we extend the theoretical framework to practical application. In machine learning, models are trained by optimizing a selected loss function that quantifies the error or likelihood of their forecasts. During training on historical data, the model learns optimal parameters by minimizing the error loss (or maximizing the likelihood function). The choice of loss function is critical because it directly shapes what patterns the model learns to capture and prioritize. Common metric functions include root mean squared error (RMSE), mean absolute error (MAE), mean absolute percentage error (MAPE), log likelihood, and the continuous ranked probability score (CRPS) for probabilistic forecasts.

Most implemented machine learning forecasting models employ one of these standard metrics as their training objective. However, a significant limitation of current practice is that loss evaluation typically focuses on one-step-ahead forecast accuracy. This limitation is suboptimal in certain situations, as optimizing for one step or a fixed horizon often results in a model that performs well at the specific horizon but deteriorates at other horizons. In fact, many practical applications require evaluating forecast quality across the entire prediction window rather than at isolated time points. For example, energy system operators may require reliable load forecasts from 1 hour ahead up to 7 days ahead simultaneously in order to make operational decisions. A loss function that treats each horizon independently can potentially lead to suboptimal real-world performance despite strong performance on standard benchmarks.

Another dimension of forecast quality that the traditional forecast evaluation metrics fail to address is stability. Consider a supply chain planner who must order inventory months in advance to meet anticipated demand. Suppose the forecast made in January predicted June demand to be 10,000 units, while an updated forecast made in February for that same June period might suddenly jump to 14,000 units, then drop to 9,500 units in the March update. Such volatility creates difficulty for decision making and planning. Procurement decisions are often irreversible, as placed orders may not be canceled easily. Unstable forecasts force planners into a difficult position: committing to large purchases based on high forecasts risks excessive inventory holding costs and potential obsolescence, while conservative ordering based on uncertain forecasts risks stockouts and lost sales. As a result, large volatility can reduce the confidence of the decision maker in the forecasts. Thus, in such situations where commitments are made based on long-horizon forecasts, stability can be a highly desirable property to have in addition to accuracy. However,

in most machine learning implementations, the objective function does not capture any notion of stability.

Our forecast AC score can address these limitations of traditional training objectives by encouraging the model to optimize for both the accuracy and stability of long horizon forecasts. When compared to models trained with traditional metrics, models trained using our multi-horizon stability aware score have the following advantages:

- Accounting for accuracy over all horizons, instead of focusing on one-step-ahead forecasts.
- Accounting for vertical stability. The forecasts targeting the same timestamp are less volatile.
- Users can easily adjust the horizon awareness of the score by assigning weights that penalize inaccuracy and instability at different horizons. In the extreme case where all but the one-step-ahead weights are set to zero, the metric is reduced to optimizing one-step-ahead forecasts.
- Users can adjust the emphasis on stability via the stability parameter λ .

In this section, we show how to set up a seasonal auto-regressive integrated model with our metric as the objective function. The trained model is compared with its counterpart trained using traditional objectives. Out-of-sample tests are performed, in which we see that models trained using our metric achieve better accuracy and stability over long horizons.

4.1. Dataset. We evaluate our method on the M4 Hourly dataset [5], a widely-used forecasting benchmark consisting of 414 hourly time series from diverse domains. This dataset was introduced in the M4 forecasting competition and has become a standard benchmark dataset for evaluating forecasting methods.

4.2. Model explanation. We employ the seasonal autoregressive integrated moving average model (SARIMA). SARIMA captures both non-seasonal and seasonal patterns in the data. Most of the time series in the M4 dataset exhibit seasonal behavior. Thus, SARIMA models serve as suitable baseline models for demonstrating the performance of our metric.

A SARIMA model is specified by seven hyperparameters: $\text{SARIMA}(p,d,q) \times (P,D,Q,s)$ where:

- p is the order of autoregression, which represents how many past values influence the current value
- d is the degree of differencing required to make the time series stationary
- q is the order of the moving average, which represents the influence of past forecast errors
- P is the seasonal autoregressive order
- D is the seasonal differencing order
- Q is the seasonal moving average order
- s is the period of the season

For computational simplicity, we restrict the moving average order q and Q to be 0. In other words, our model takes the form of $\text{SARIMA}(p,d,0) \times (P,D,0,s)$. We will refer to this model as SARI in the paper. The mathematical representation of our model is given by

$$(20) \quad \Phi(L^s)\phi(L)(1-L^s)^D(1-L)^d y_t = \epsilon_t$$

where L is the lag operator, which shifts the time series backward by one step, i.e. $Ly_t = y_{t-1}$. The term $\phi(L)$ refers to the autoregressive polynomial. That is, given autoregressive coefficients ϕ_1, \dots, ϕ_p ,

$$\phi(x) = 1 - \phi_1 x - \phi_2 x^2 - \dots - \phi_p x^p.$$

Similarly,

$$\Phi(x) = 1 - \Phi_1 x - \dots - \Phi_P x^P,$$

For a fixed set of hyperparameters (p, d, P, D, s) , the model is determined by the corresponding autoregressive and seasonal autoregressive coefficients ϕ_j, Φ_j . This simple structure allows us to easily set up optimization procedures to find the optimal coefficients under our metric.

4.3. Training. For each time series in the M4 Hourly dataset, we perform the following training and evaluation procedure:

Data Splitting. We partition each series into training and test sets using a 60-40 split ratio. Given a time series of length T , the training set consists of the $[0, 0.6T]$ observations and the remaining observations go into the test set for out-of-sample evaluation.

Hyperparameter Selection. We employ the auto-ARIMA algorithm from the `pmdarima` library [9] to automatically determine the optimal SARI hyperparameters (p, d, P, D, s) . The auto-ARIMA performs a stepwise search over the hyperparameter space. The Akaike Information Criterion (AIC) is used as the metric for comparison, which accounts for both model fit and model complexity. This automated hyperparameter selection procedure ensures that our models are tuned to the specific pattern of each time series in the dataset.

Traditional Model Fitting. Using the hyperparameters found by auto-ARIMA, we create a traditional SARI model using `statsmodel` library [8]. The model is fitted on the training set using maximum likelihood estimation (MLE) with standard one-step-ahead forecast error minimization as the optimization objective. This serves as a benchmark for comparing with the optimized model under our novel metric.

Differentiable Model Fitting. We start by creating a differentiable SARI model with the same hyperparameters as the traditional model. The autoregressive coefficients are treated as learnable parameters. They are initialized as random floats in the interval $(-1, 1)$.

Our innovation lies in using our multi-horizon stability-aware forecast AC score as the objective for learning the autoregressive coefficients. In each training epoch, we generate rolling forecasts on the training data. Specifically, the rolling forecast starts from the timestamp whose index is equal to the minimum required history length, which is in turn equal to the maximum lag of the SARI model. We produce H -step-ahead forecasts for each valid forecast origin. The multi-step forecasts are simulated via the equation (20). The forecast ensembles are stored in the form of (2). The forecast origins are processed in batches of size 32 for computational efficiency.

Next, we compute the loss by comparing the forecast ensemble against the true outcomes according to our proposed metric (14) and (16). The horizon aware weight w was set to be linear

$$w(j) = 1 - \frac{j}{h}$$

and later normalized to sum up to 1. This weight encourages the model to pay more attention to optimizing accuracy and stability of the short-range forecasts, while maintaining a reasonable level of awareness of the quality of long-range ones. The stability multiplier λ is set to 0.5.

Since the setup of the differentiable model as well as the entire forecast generating process are implemented with PyTorch, the whole process is differentiable. We backpropagate to compute the gradient of the loss function $\nabla_{\phi, \Phi} S_{AC}(F|Z)$ where ϕ, Φ refer to all of the autoregressive coefficients. We employed the AdamW optimizer with an initial learning rate of 0.05. A ReduceLRonPlateau scheduler was employed to reduce the learning rate by a factor of 0.5 when the loss plateaus for 10 consecutive epochs. We set the seed for PyTorch and Numpy operations to 42 for reproducibility.

After the training is completed, we verify that the SARI model with the learned coefficients are stationary by examining the roots of the autoregressive polynomial

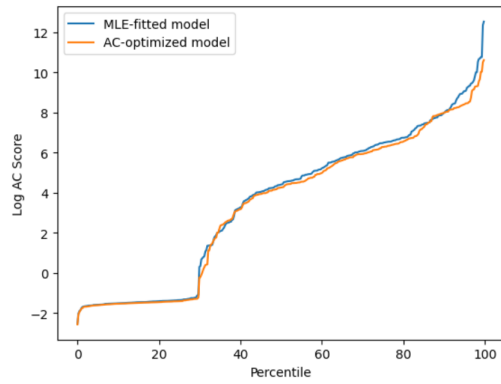
$$(21) \quad \phi(L)\Phi(L^s)$$

It is a well-known fact that a model is stationary if all roots of (21) lie outside the unit circle $|z| = 1$.

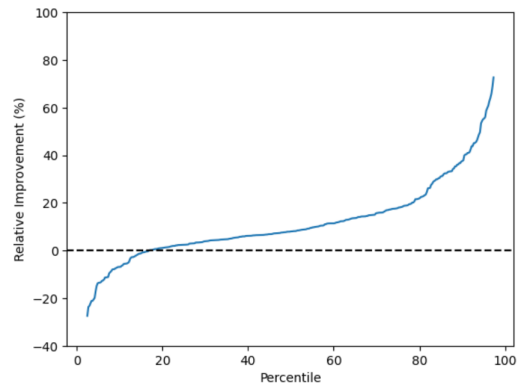
Out-of-sample Testing. In order to validate the results on unseen data, we perform out-of-sample tests. We use both of the traditionally trained model and the model trained with our metric to generate rolling forecasts on the test set, for each time series in the dataset. The models we used in the experiments generate and evaluate point forecasts, which can be viewed as degenerate probability distributions with all mass concentrated at a single value. With this simplification we can demonstrate the metric’s effectiveness in improving multi-horizon accuracy and stability without the additional complexity of generating full predictive distributions.

4.4. Results. We evaluated the performance of our AC-optimized SARI model against the traditionally trained model on 414 time series in the M4 dataset. Overall, results show that our custom optimization yields substantially improved stability, while often with minimal accuracy trade-offs, whether measured by one-step-ahead error (using MAPE) or multi-step-ahead error and stability (using forecast AC Score). Figure 2 provides a comprehensive comparison of the MLE-fitted and AC-optimized models in terms of their forecast AC score (14), accuracy score (9) and stability score (13). Specifically, figures 2a, 2c, and 2e display these log transformed version of these scores at each percentile (log transformation is applied due to the large variation in original scales across time series). Figures 2b, 2d, and 2f show the percentile distribution of relative improvements achieved by the AC-optimized model over the MLE-fitted model for each of the three metrics. We quote some statistics of the relative improvement in Table 1.

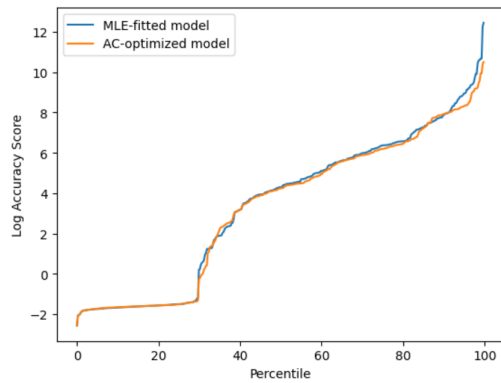
Enhanced Forecast Stability. The ultimate purpose of our metric is to guide the model to output more stable forecasts. This has been achieved in the out-of-sample tests. Figure 3 displays forecasts generated from multiple forecast origins, all targeting the same future timestamp. The traditionally trained SARI model exhibits substantial variation across these forecasts. It updates the forecast by considerable amounts when moving through forecast origins, and often completely reverts its previous update after another step. In contrast, our AC-optimized model



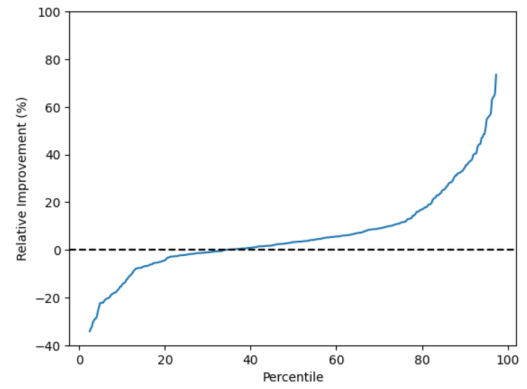
(A) Log AC Score



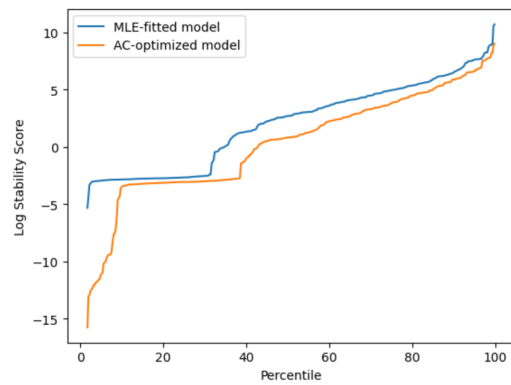
(B) Relative Improvement of AC Score



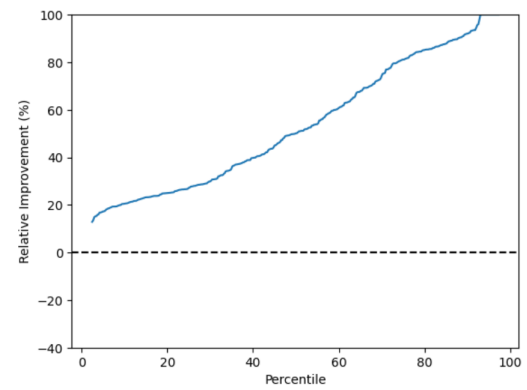
(C) Log Accuracy Score



(D) Relative Improvement of Accuracy Score



(E) Log Stability Score



(F) Relative Improvement of Stability Score

FIGURE 2. Comparison of metrics at log scale

TABLE 1. Relative improvement of AC-optimized model over MLE-fitted model

Statistic	AC Score Improvement	Accuracy Score Improvement	Stability Score Improvement
25% Percentile	2.38%	-2.08%	27.06%
50% Percentile (Median)	7.94%	3.18%	50.00%
75% Percentile	17.72%	11.09%	81.00%

produces remarkably consistent predictions with forecasts issued from different origins converging to similar values as the traditionally trained model predicts when approaching target timestamps. Figure 3 visualizes such scenarios where the x-axis represents the forecast origins and the y-axis represents the forecast values made at these origins targeting the same target timestamp.

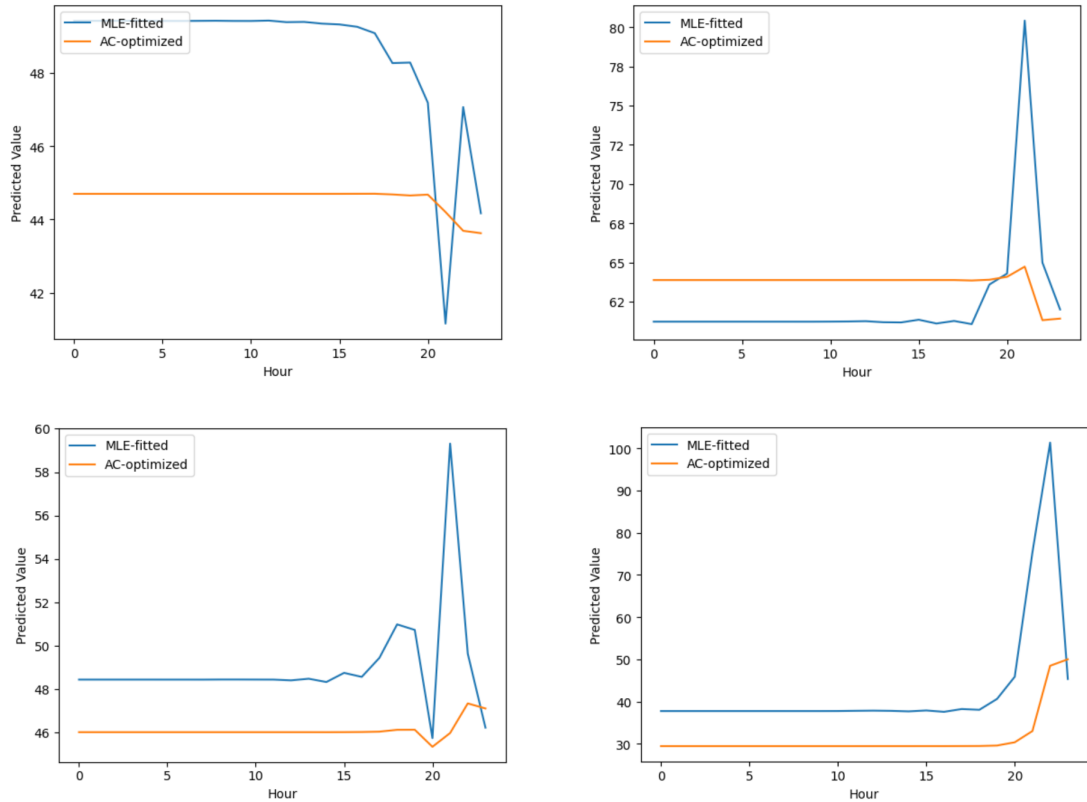


FIGURE 3. Examples illustrating superior vertical stability.

To quantify the improvement in forecast stability in an alternative way, we compute the sample variance of the forecasts targeting the same future timestamp

across different forecast origins. Specifically, for each target timestamp t in the test set, we collect all forecasts $\hat{y}_{t|s}$, $t-h \leq s \leq t-1$ and calculate their variance

$$(22) \quad s_{\text{vertical}}^2(t) = \frac{1}{h-1} \sum_{s=t-h}^{t-1} (\hat{y}_{t|s} - \bar{\hat{y}})^2$$

where $\bar{\hat{y}}$ is the average of forecasts $\hat{y}_{t|s}$ over $t-h \leq s \leq t-1$. We then average over all target timestamps t . This mean value measures the volatility of vertical forecasts. Lower values indicate that predictions for the same future point are stable throughout forecast origins. We then average this mean variance across all test time series to obtain an overall stability measurement. As a result, the vertical volatility (represented by (22)) of the AC-optimized model is only 8.9% of that of the MLE-fitted model, with the former output forecasts whose variance is 4.1 and the latter's forecasts having a much greater variance equal to 45.7.

Accuracy Trade-off at Different Horizons. Two natural concerns when using the forecast AC score are

- (1) Whether improving stability comes at the cost of forecast accuracy.
- (2) Whether aiming at multi-step-ahead comes at the cost of accuracy at one-step-ahead.

To evaluate these trade-offs comprehensively, we employ two complementary evaluation strategies. We begin by assessing performance using our forecast AC score as it directly reflects the optimization objective and both the accuracy and stability of multi-step ahead. We then supplement this with horizon-specific MAPE analysis for two reasons: (1) MAPE provides an intuitive, scale-independent accuracy measure familiar to most practitioners and allows for more straightforward interpretation; (2) examining individual horizons allows us to demonstrate that our multi-horizon optimization does not drastically sacrifice one-step-ahead forecast quality, which is still an important objective for most forecasting works.

The AC-optimized model achieved improved forecast AC score for 83% of the tested series, with significantly improved stability as shown in Figure 2f. In exchange for the stability improvement, the AC-optimized model generated slightly less accurate forecasts for approximately 25% of the time series (the first quantile in Figure 2d). However, the combined AC score still improved for the majority of series, demonstrating that stability gains outweighed the modest accuracy losses for these cases.

Next we measure the trade-off between the one-step-ahead accuracy and multi-step-ahead accuracy plus stability by evaluating the MAPE of the one-step-ahead forecasts. Figure 4 presents the percentage MAPE improvement of the AC-optimized model relative to the traditional MLE-fitted model across forecast horizons, along with 50% confidence intervals. The comparison is evaluated with the percentage improvement in terms of MAPE, as in equation (23)

$$(23) \quad \% \text{ Improvement} = \frac{\text{MAPE}_{MLE} - \text{MAPE}_{AC}}{\text{MAPE}_{MLE}}.$$

At the one-step-ahead horizon, our AC-optimized model produces moderately less accurate forecasts, with its MAPE 7.5% worse compared to that of the traditional model at 50% percentile. However, this short-term accuracy cost is quickly recovered: starting at a horizon equal to 2, our model consistently outperforms the traditional approach in both accuracy and vertical stability. The performance gap

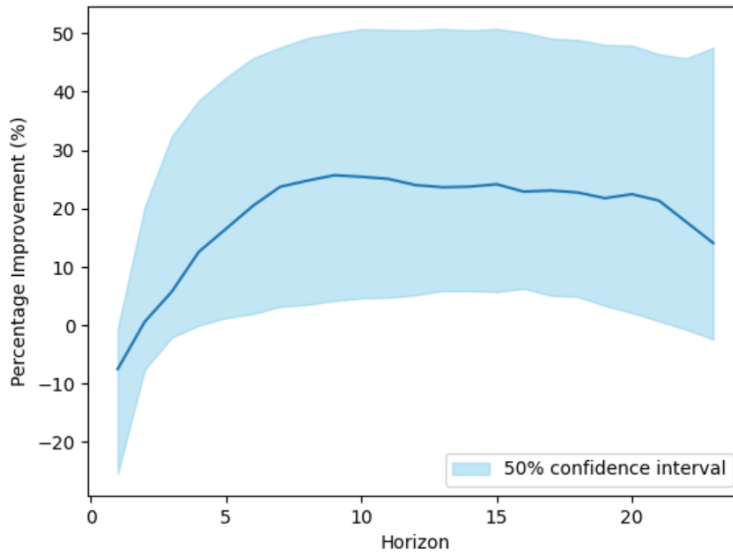


FIGURE 4. Percentage MAPE improvement of the AC-optimized model over the traditional MLE-fitted model.

widens substantially as the forecast horizon extends. For longer horizons, our AC-optimized model achieves up to a 26% better MAPE compared to the traditional model. This pattern demonstrates that, while traditional MLE training excels at optimizing one-step-ahead predictions, it fails to generalize effectively to longer horizons. In contrast, our multi-horizon approach is able to generate much more accurate long-horizon forecasts with only a relatively small loss of one-step-ahead forecast accuracy. This trade-off can prove useful for practical decision-making where medium and long term planning decisions are typically important.

Remark. One may notice that (23) starts to decrease after horizon equal to 12. This is due to our choice of horizon discounting weights, which is linear in horizon and assigns more importance to shorter horizon compared to longer horizon. The improvement remains positive, indicating that the AC-optimized model still outperforms the MLE-fitted model to a lesser extent at these horizons.

One-Step-Ahead Accuracy Distribution. At one step ahead, the AC-optimized model trades off accuracy to some extent in exchange for longer horizon accuracy and stability. To provide a more detailed picture of this trade-off, we analyze the distribution of performance differences between the two approaches. Table 2 provides detailed statistics that compare the performance of two models measured by the one-step-ahead MAPE. Figure 5 is a histogram of the relative MAPE improvement (evaluated as in (23)) across all test series for one-step-ahead forecasts. The distribution reveals that while the traditional model generally performs better at this horizon, the magnitude of improvement varies considerably across series. The median improvement (50th percentile) is approximately -7.5%, indicated by the middle vertical line, suggesting that for a typical series, the traditional model achieves modestly better one-step-ahead accuracy. The first quartile consists of 25% of the tested time series on which the AC-optimized model experienced equal

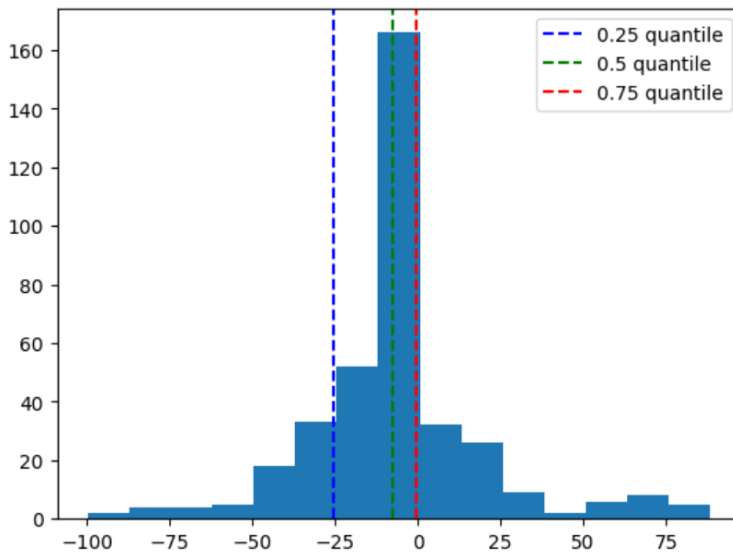


FIGURE 5. Percentage forecast MAPE improvement (%) of MLE-fitted model relative to AC-optimized model at one step ahead.

to or greater than 25.4% degradation in terms of MAPE. The third quartile (75th percentile) is approximately -0.5%, indicating that the AC-optimized model showed practically no degradation or improvement for 25% of the test series.

TABLE 2. Model comparison using MAPE.

Statistic	MLE-fitted MAPE	AC-optimized MAPE	% Improvement
25% Percentile	0.0025	0.0028	-25.4%
50% Percentile (Median)	0.0185	0.0321	-7.5%
75% Percentile	0.2055	0.2129	-0.5%

4.5. Sensitivity to Time Discounting Weights. We complement our discussion of weight functions in section 3.5 and assess their influence on optimizing multi-horizon accuracy and stability. We repeat the experiments using three additional weight types: uniform ($w(h) = 1$), exponential ($w(h) = e^{-\frac{5}{24}h}$), and hyperbolic ($w(h) = \frac{1}{1+h}$), each normalized to sum up to 1.

Figure 6 presents the log mean vertical variance of all time series, sorted in ascending order and mapped to percentile. The mean vertical variance is defined in the same way as 22 and provides a comparison between the stability of forecast generated by models trained using each weight type. The log transformation is applied to adjust the scale. While all schemes improve stability, uniform weights produced the most stable forecasts at almost every percentile, followed by linear weights, then exponential and hyperbolic weights. This result is consistent with the heuristic that uniform weight assigns equal weights to short and long horizons, coercing the forecasts to stay stable. The other weights decay for longer horizon,

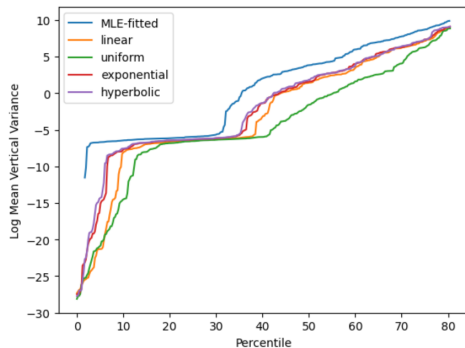


FIGURE 6. Effect of Weight on Optimizing Stability

with the rate of decay from slowest to fastest: linear, hyperbolic, exponential. Suppose one sets the rate of decay to approach infinity, which results in the weight converging to $w(h) = \delta(h = 1)$ after normalization. This limit case is exactly equivalent to training the model based on one-step-ahead performance. Hence as the weight decays faster from uniform to exponential, the vertical variance increases and approaches what is learned by the one-step-ahead MLE model.

5. CONCLUSION

In this paper, we introduced a novel evaluation score, the forecast accuracy and coherence (AC) score, for multi-horizon time series forecasting that accounts for both forecast accuracy and stability across prediction horizons. Unlike traditional metrics that focus solely on point forecast accuracy at individual horizons, our metric provides an assessment of forecast quality by simultaneously measuring how well predictions match observed values and how consistently models predict the same future events from different forecast origins.

Our metric is built upon the energy score and energy distance. It is highly customizable, as one can specify relative weights to discount forecasts at longer horizons based on problem-specific needs, and can adjust the relative importance of stability with respect to accuracy through the stability multiplier parameter. This makes the metric applicable across diverse forecasting contexts, from applications where stability is paramount (such as capacity planning and resource allocation) to those where accuracy at specific horizons takes precedence.

To validate the utility of the forecast AC score, we implemented it as a differentiable objective function for training SARI models. We performed experiments on the M4 Hourly benchmark dataset. As a result, models trained using our metric yield substantial improvements over traditionally trained models in terms of multi-horizon accuracy and stability. In terms of stability, the AC-optimized model generated out-of-sample forecasts with 8.9% vertical volatility relative to that of MLE-fitted model. On the accuracy side, the accuracy of forecasts targeting middle to long horizons are substantially improved for the AC-optimized model. While the one-step-ahead forecasts suffered a 7.5% degradation in MAPE, forecasts targeting all subsequent horizons experienced improved accuracy, up to 26% measured

by MAPE. This indicates that our metric is capable of training models that produce more stable and accurate multi-step forecasts at relatively small cost of the one-step-ahead forecasts.

6. FUTURE DIRECTIONS

In the final section of the paper, we discuss some potential directions for extending our current work.

6.1. Application to more advanced models. Our current implementation excludes moving average (MA) terms from the SARIMA specification. This restriction addresses a computational challenge: in a differentiable implementation, MA components require forecast error history, which depends on forecasts from previous training epochs. This creates deep computational graphs that significantly increase memory requirements and training time. Future work will incorporate MA components through techniques such as error approximations to reduce computational cost.

We additionally plan to evaluate the AC score on modern forecasting models including DeepAR, Temporal Fusion Transformers, and N-BEATS. These experiments will provide a full picture of the metric’s applicability beyond classical statistical models.

6.2. Adjusting for Natural Variance Shrinkage. It is well known that forecast variance typically shrinks naturally as the horizon decreases and the target time approaches. To isolate true instability from this natural variance reduction, one can account for the expected evolution of uncertainty along the path and remove its contribution when computing the stability term. This ensures that the stability metric captures unexpected fluctuations rather than predictable variance shrinkage.

6.3. More Complex Forecasting Architectures. While we have demonstrated the utility of our metric with the SARI model, the metric can also be utilized as an objective function in training more complex models.

6.4. Adjusting Penalties for “Justified” Revisions. While forecast stability is desirable in many applications, accuracy typically takes precedence when these objectives conflict. Stability is primarily valued as a tie-breaker when comparing forecasts of similar accuracy levels. For example, consider forecasts for a temperature-sensitive product such as winter apparel. A sudden temperature drop increases demand, prompting the forecaster to revise predictions upward. Although this revision is subject to a stability penalty, it is well-justified because it improves forecast accuracy by incorporating relevant new information. Our current metric penalizes all forecast revision equally, regardless of whether the revisions improve accuracy. Future work could refine the stability penalty to distinguish between “justified revisions” that genuinely improve forecast accuracy and “gratuitous revisions” that do not enhance predictive performance. This extension would reward forecasters for appropriately updating their predictions in response to new information while still penalizing erratic behavior that reflects model instability rather than genuine learning from data. One approach might involve calculating an “optimal revision” that achieves the same accuracy as the current revision, but at minimal instability, and then assigning a penalty based on the deviation from this optimal revision.

REFERENCES

1. E. Genov, J. Ruddick, C. Bergmeir, M. Vafaeipour, T. Coosemans, S. García, and M. Messagié, *Predict. Optimize. Revise. On Forecast and Policy Stability in Energy Management Systems*, ArXiv preprint (2025).
2. T. Gneiting and A. E. Raftery, *Strictly Proper Scoring Rules, Prediction, and Estimation*, Journal of the American Statistical Association **102** (2007), no. 477, 359–378.
3. R. Godahewa, C. Bergmeir, Z. Erkin Baz, C. Zhu, Z. Song, S. García, and D. Benavides, *On forecast stability*, International Journal of Forecasting **41** (2025), no. 4, 1539–1558.
4. S. Klee and Y. Xia, *Measuring Time Series Forecast Stability for Demand Planning*, ArXiv preprint (2025), 1–6, arXiv:2508.10063 [cs.LG].
5. Spyros Makridakis, Evangelos Spiliotis, and Vassilios Assimakopoulos, *The M4 Competition: Results, findings, conclusion and way forward*, International Journal of Forecasting **34** (2018), no. 4, 802–808.
6. K. Pritularga and N. Kourentzes, *Forecast Congruence: A Quantity to Align Forecasts and Inventory Decisions*, Management Science (2024), no. 1, 8–10.
7. Maria L Rizzo and Gábor J Székely, *Energy distance*, Wiley Interdisciplinary Reviews: Computational Statistics **8** (2016), no. 1, 27–38.
8. Skipper Seabold and Josef Perktold, *statsmodels: Econometric and statistical modeling with python*, 9th Python in Science Conference, Austin, TX, 2010.
9. Taylor G. Smith et al., *pmдарima: ARIMA estimators for python*, (2017), Version 2.0.0.
10. M. Zanotti, *The effects of retraining on the stability of global models in retail demand forecasting*, ArXiv preprint arXiv:2506.05776 (2025).

Email address: `c.ma@causify.ai`

Email address: `g.pomazkin@causify.ai`

Email address: `gp@causify.ai`

Email address: `paul@causify.ai`